ChemPubSoc Europe

DOI: 10.1002/open.201800191

Open Access ChemistryOPEN Full Papers

Half-Sandwich Metal-Catalyzed Alkyne [2+2+2] Cycloadditions and the Slippage Span Model

Marco Dalla Tiezza,[a] F. Matthias Bickelhaupt,*[b, c] and Laura Orian*[a]

Half-sandwich Rh^{I} compounds display good catalytic activity toward alkyne [2+2+2] cycloadditions. A peculiar structural feature of these catalysts is the coordination of the metal to an aromatic moiety, typically a cyclopentadienyl anion, and, in particular, the possibility to change the bonding mode easily by the metal slipping over this aromatic moiety. Upon modifying the ancillary ligands, or proceeding along the catalytic cycle, hapticity changes can be observed; it varies from η^5, if the five metal–carbon distances are identical, through $\eta^3+\eta^2$, in the presence of allylic distortion, and η^3, in the case of allylic coordination, to η^1, if a σ metal–carbon bond forms. In this study, we present the slippage span model, derived with the aim of establishing a relationship between slippage variation during the catalytic cycle, quantified in a novel and rigorous way, and the performance of catalysts in terms of turnover frequency, computed with the energy span model. By collecting and comparing new data and data from the literature, we find that the highest performance is associated with the smallest slippage variation along the cycle.

1. Introduction

Metal-catalyzed [2+2+2] cycloadditions are important reactions for the synthesis of cyclic and polycyclic compounds such as benzene, pyridine, and their derivatives starting from unsaturated molecules such as alkynes, alkenes, and nitriles.[1] Half-metallocene fragments, in which the metal is coordinated to an aromatic moiety and the electronic saturation is ensured by ancillary ligands (e.g. CO, phosphines, etc.), are largely employed. An important advantage of these catalysts is the facility of displacement of the metal from the centroid of the coordinated aromatic ring, called slippage, which can also change dramatically along the catalytic cycle in some cases. Slippage has important effects on the structure and energy of the intermediates and transition states and, thus, affects reactivity. The most studied organometallic half-sandwich compounds for the [2+2+2] cycloadditions of alkynes are those containing the ubiquitous cyclopentadienyl anion (Cp, Scheme 1A) and the indenyl anion (Ind, Scheme 1B). Recently, the diheteroaromatic rings 1,2-azaborolyl (Ab, Scheme 1C) and 3a,7a-azaborindenyl (Abi, Scheme 1D) were also tested in silico in Rh^{I} half-sandwich catalysts.[2–13] The idea was to design catalysts for the [2+2+2] cycloaddition of alkynes with enhanced metal slippage promoted by the low symmetry of these anions, which are isoelectronic to the parent hydrocarbons Cp and Ind, respectively.

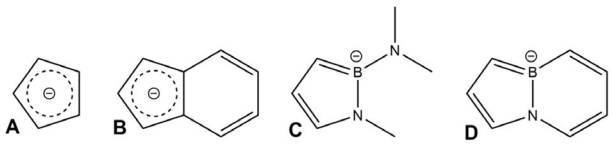

Scheme 1. Aromatic ligands of the half-sandwich catalysts: A) cyclopentadienyl anion (Cp, $C_5H_5^-$), B) indenyl anion (Ind, $C_9H_7^-$), C) 1,2-azaborolyl anion (Ab, $C_6H_{12}BN^-$), and D) 3a,7a-azaborindenyl anion (Abi, $C_7H_7BN^-$).

Cyclotrimerizations are strongly exergonic processes that are highly disfavored by entropic factors, and so, their activation energy is typically quite high (60–80 kcal mol^{-1}).[14] The first evidence of a Ni^{II}-catalyzed cyclotrimerization, based on the 1,3,5,7-cyclooctatetraene (cot) ligand, was reported by Reppe et al.[15] Pyridine synthesis from alkynes and nitriles, driven by CpCo as the catalyst, was highlighted in the pioneering studies of Wakatsuki and Yamazaki in 1973,[16,17] followed by the work of Vollhardt et al.[18,19] and Bönnemann et al.[20,21] in the 1980s. For many years, cobalt-based catalysts remained on top in terms of efficiency. To the best of our knowledge, the first Rh^{I}

[a] M. Dalla Tiezza, Prof. Dr. L. Orian
Dipartimento di Scienze Chimiche
Università degli Studi di Padova
Via Marzolo 1 35129 Padova (Italy)
E-mail: laura.orian@unipd.it

[b] Prof. Dr. F. M. Bickelhaupt
Department of Theoretical Chemistry and
Amsterdam Center for Multiscale Modeling (ACMM)
Vrije Universiteit Amsterdam
De Boelelaan 1083, 1081 HV Amsterdam (The Netherlands)
E-mail: f.m.bickelhaupt@vu.nl

[c] Prof. Dr. F. M. Bickelhaupt
Institute for Molecules and Materials (IMM)
Radboud University
Heyendaalseweg 135, 6525AJ Nijmegen (The Netherlands)

Supporting Information and the ORCID identification number(s) for the author(s) of this article can be found under: https://doi.org/10.1002/open.201800191.

catalyst ever reported and used in the cycloaddition of alkynes was a neutral rhodacyclopentadiene/arsine complex in 1968.[22] Afterwards, Booth et al.[23] and Ingrosso et al.[24,25] described a variety of Rh^{I} half-sandwich complexes that were synthesized and tested to understand how the overall cyclotrimerization yield could be trimmed and optimized. In agreement with the observations of Wakatsuki and Yamazaki for Co catalysts, $[Rh(\eta^5\text{-}C_5H_5)L_n]$ ($L = C_2H_4$, CO, PR_3; L_2 = 1,5-cyclooctadiene) proved to be very promising; L_n refers to a bunch of common ligands used in inorganic catalysis, such as C_2H_4, carbonyl (CO), tertiary phosphines (PR_3) or a bulky group such as 1,5-cyclooctadiene (cod). These [2+2+2] cycloadditions take place in toluene at reflux, but efforts have been made to test different conditions with the aim of tuning the overall rate. Importantly, analogous reactions in aqueous solution were also recently reported.[26,27] Unfortunately, in all of these experimental studies, a rigorous mechanistic investigation was never performed and only a few hypotheses were proposed. For example, Ingrosso and co-workers discussed the coordination of a nitrile to the metallacycle intermediate in terms of two possibilities: either end on, that is, through the formation of a metal–N σ bond, or side on, that is, through an interaction metal–CN π system. The lack of mechanistic details about [2+2+2] cycloadditions catalyzed by Rh^{I} compounds is also emphasized in the rather recent book "Transition-Metal-Mediated Aromatic Ring Construction" by Ken Tanaka,[1] who writes "…although mechanistic aspects of these reactions attract interest, only a few studies have been reported in specific catalysts and substrates…".

The mechanistic investigation by Albright and co-workers[14] on CpCo-catalyzed acetylene cyclotrimerization to benzene is undoubtedly pioneering. They analyzed the potential energy surface of the whole catalytic cycle, mainly with the Hartree–Fock (HF) method, and thus missed some intermediates because of a lack of electron correlation, although all the relevant species were thoroughly discussed. A few years later, Calhorda and Kirchner and co-workers described the CpRuCl-catalyzed [2+2+2] cycloaddition of acetylene to give benzene by using DFT methods.[28] In 2007, the same reaction, catalyzed by CpRh as well as by IndRh fragments, was analyzed.[29] The authors discussed different paths for the synthesis of benzene and also tackled the CpRh-catalyzed synthesis of 2-methylpyridine from acetylene and acetonitrile. In 2008, the same authors explained the end-on/side-on linkage isomerism of a generic nitrile coordinated to a rhodacycle; this is an elementary step that was first postulated by Ingrosso[24] in the CpRh-catalyzed synthesis of 2-methylpyridine.[30] Another interesting investigation of reaction paths was performed by Koga et al.[31] on Co-based half-sandwich catalysts, taking into account the stability of the triplet electronic state of the cobaltacycle formed during the first step, that is, the oxidative coupling. The CpIr catalyst has also been studied in silico, although interest in iridium has remained quite limited relative to interest in other metals such as Co, Rh,[32,33] and Ru.[28] The advantage of CpCo, with respect to heavier CpRh, in the initial oxidative coupling to form the metallacyclopentadiene was rationalized very recently and was ascribed to smaller slippage variation of the lighter metal along the reaction path.[34]

One puzzling aspect emerging in the abovementioned DFT mechanistic study of 2007,[29] in which CpRh and IndRh were compared, is the lack of an indenyl effect, consisting of "enhanced kinetic performance" of the latter fragment, which, due to the presence of the benzene ring fused with the Cp moiety, allows easier metal slippage. This unexpected computational result led to the hypothesis of a different mechanism[35] inspired by the experimental work of Booth et al.,[23] in which the real catalysts are L–CpRh and L–IndRh (L = CO).

In the present work, we propose the slippage span model to establish a relationship between the structure, the energetics, and the activity of CpRh, IndRh, AbRh, and AbiRh employed in the [2+2+2] cycloaddition of acetylene to give benzene and the [2+2+2] cocycloaddition of acetylene/acetonitrile to give 2-methylpyridine, likely transferable to analogous catalytic fragments. The novelty addresses the whole catalytic cycle rather than the key elementary steps, such as the initial oxidative coupling. To this purpose, the energy profiles of a few more catalytic cycles were calculated, whereas others were taken from the literature. In addition, in selected cases, a comparison with CpCo and CpIr catalysis is made to assess the role of the metal center.

2. Results and Discussion

The main goal of this work was to relate the chemical reactivity of the studied half-sandwich catalysts to their relevant changes in geometry during the cyclotrimerization process. First, we investigated in silico the potential energy surfaces (PESs) of the [2+2+2] cycloaddition of acetylene to give benzene and the cocycloaddition of acetylene/acetonitrile to give 2-methylpyridine catalyzed by half-sandwich group 9 metal (Co, Rh, Ir) fragments; the results are presented in the first two paragraphs of this section. Using the energy span model, the turnover frequency (TOF) values of the catalytic cycles were computed, and the trends are discussed in the third paragraph. In particular, the observation that lower TOF values are associated to low-symmetry and/or more largely slipped catalysts, we define a novel slippage parameter, the label-independent slippage parameter (LISP), which accounts for nonsymmetric metal displacements from the centroid of the coordinated aromatic ring. It emerges that the larger the slippage span, ΔLISP, defined as the difference between the maximum and minimum hapticity value measured in a cycle, the lower the TOF. This is the essence of the slippage span model, which is intended as a tool to design efficient metal half-sandwich catalysts for the [2+2+2] cycloaddition of alkynes; this is discussed in the last two paragraphs of this section.

2.1. Group 9 Metal-Catalyzed [2+2+2] Cycloaddition of Acetylene to Give Benzene: Reaction Mechanism and PES

The simplest metal-catalyzed [2+2+2] cycloaddition converts three molecules of acetylene into benzene. Over the years, several mechanisms have been proposed and analyzed (Scheme 2). It is consolidated that the path starts from a catalyst precursor $[ZML_n]$ (Z: Cp, Ind, Ab, Abi; M: Co, Rh, Ir; L: C_2H_4,

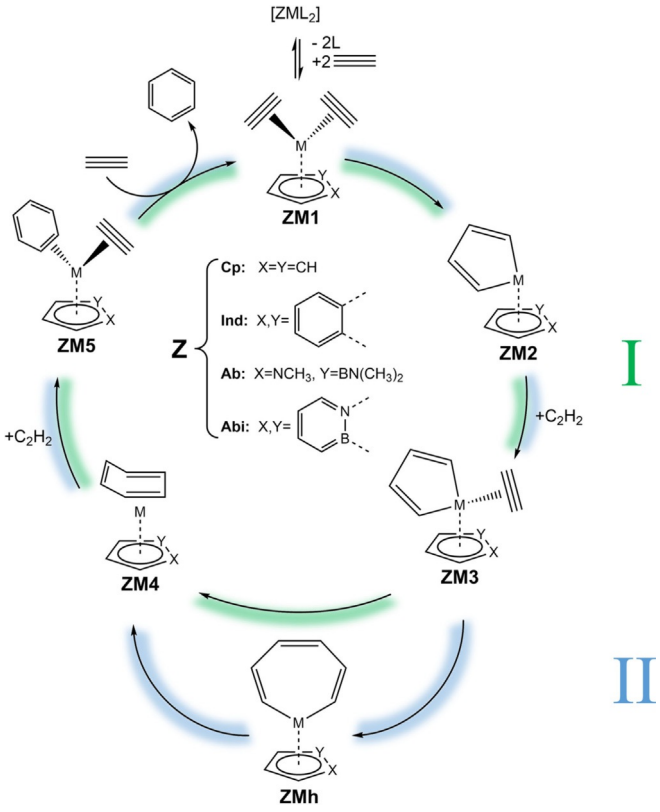

Scheme 2. Mechanism for the [2+2+2] cycloaddition of acetylene to give benzene catalyzed by a half-sandwich metal fragment CpM (M = Co, Rh, Ir) and ZRh; (L = C_2H_4, CO, PH_3).

CO, PR_3; L_2: cod) in which the ancillary ligands L are replaced by two acetylene molecules in a photo- or thermochemical process.[29] By oxidative coupling of the two acetylene molecules, the very stable 16-electron ZM2 intermediate forms. From the reaction environment, an acetylene molecule easily coordinates to the metal center in an η^2 fashion to restore a stable 18-electron configuration (ZM3). The synchronous formation of two C–C bonds leads to the formation of an unusual bent six-membered ring in ZM4 (Scheme 2 I): this arrangement allows benzene to remain coordinated to the metal, satisfying the 18-electron rule. Then, cleavage occurs by stepwise addition of two acetylene molecules to regenerate ZM1. An interesting variation proposed by Schore[36] predicts the formation of a metallacycloheptatriene (ZMh) upon insertion of the third acetylene molecule in one of the two metal–carbon bonds of the five-membered ring of ZM2; then, benzene formation occurs by reductive elimination (Scheme 2 II). This last step requires a high activation energy, and thus, this path can be ruled out from the mechanism, as explained in detail in Ref. [29] An alternative path was proposed by Booth and coworkers,[23] and it relies on the hypothesis that, at the beginning, acetylene replaces only one of the two ligands L of the catalyst precursor. This leads to a significantly different mechanism[35] characterized by peculiar intermediates (Scheme 3) such as rhodabicyclo[3.2.0]heptatriene and rhodaheptatetraene, which are structurally similar to intermediates found in the catalytic mechanism of CpRuCl.[28] Starting from ZM2, an al-

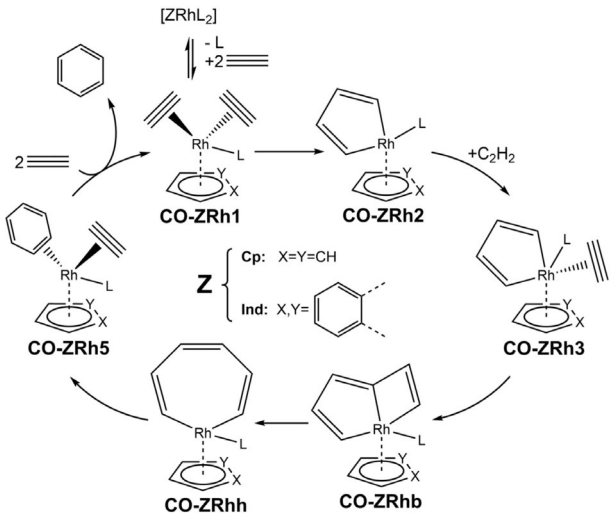

Scheme 3. Mechanism for the [2+2+2] cycloaddition of acetylene to give benzene catalyzed by a half-sandwich Rh^I fragment in the hypothesis that an ancillary ligand (L = CO) remains bonded to the metal throughout the whole catalytic cycle.[35]

ternative mechanism in the triplet state might take place: in fact, Dahy et al. showed that the triplet state cobaltacycle was more stable than the singlet one, that is, by 16.6 kcal mol^{-1}.[37] Then, the catalytic cycle continues on the triplet surface until the second crossing point, which corresponds to the intermediate ZM4, although in Dahy's mechanism the preceding coordination of acetylene implies two different intermediates. ZM4 is more stable in the triplet state, but this electronic change implies also a variation in the coordination of benzene from η^4 to η^6. The last crossing point leading again to the singlet surface is not reported in Ref. [37] but should correspond to the coordination of the two acetylene molecules to displace benzene.

The PESs for benzene synthesis (Scheme 2 I) catalyzed by CpCo and CpIr were calculated at ZORA-BLYP/TZ2P, that is, the same level of theory as that used in the literature in the cases of CpRh, IndRh,[35] AbRh, and AbiRh.[38] Only singlet states were considered.

At a glance, the CpCo-catalyzed cycle shows the flattest PES, whereas the AbRh- and AbiRh-catalyzed ones show the largest energy spans (Figure 1). This already gives a qualitative idea of the catalysts' performance: Co-based catalysts (in this case CpCo) are better suited for cyclotrimerizations than analogous Rh- and Ir-based complexes, in agreement with the experimental findings. The loss of performance in the presence of more asymmetric aromatic ligands such as Ab and Abi, as reported in 2013,[38] is also evident.

2.2. Group 9 Metal-Catalyzed [2+2+2] Cycloaddition of Acetylene/Acetonitrile to Give 2-Methylpyridine: Reaction Mechanism and PES

The mechanism leading to 2-methylpyridine was studied as well. Early experimental studies[20,24] report catalyzed cyclotrimerizations with pyridine or pyridine derivatives as products if the acetylene pressure is partially replaced by acetonitrile or

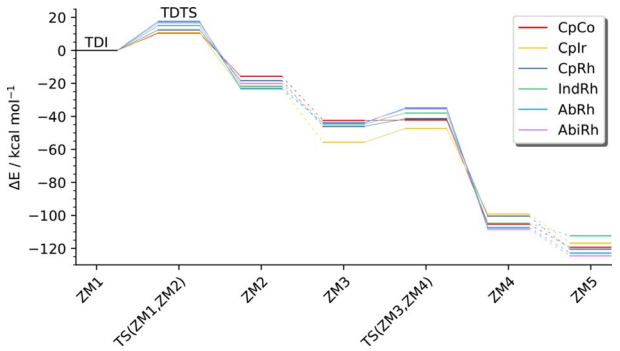

Figure 1. Energy profile for the metal-catalyzed [2+2+2] cycloaddition of acetylene to give benzene (level of theory: ZORA-BLYP/TZ2P). The mechanism is shown in Scheme 2I.

molecules with a CN functional group. The mechanistic details differ from those of benzene synthesis, because the forming π system is not symmetric (due to the presence of N), and thus, more intermediates are found. The reaction path for the CpRh-catalyzed [2+2+2] cocycloaddition to give 2-methylpyridine,[29] used in this work as a model mechanism, is characterized by nine intermediates and six transition states (Scheme 4).

The initial part of the cycle is identical to that for the [2+2+2] cycloaddition of acetylene to give benzene, as the initial coordination of two acetylene molecules is thermodynamically more favored than the coordination of one acetylene molecule and one nitrile molecule.[39] The highest energy point of the whole cycle, TS(ZM1,ZM2), is reached once the five-membered metallacycle ZM2 forms. Nitrile coordination takes place over two steps: initially, the terminal nitrogen atom

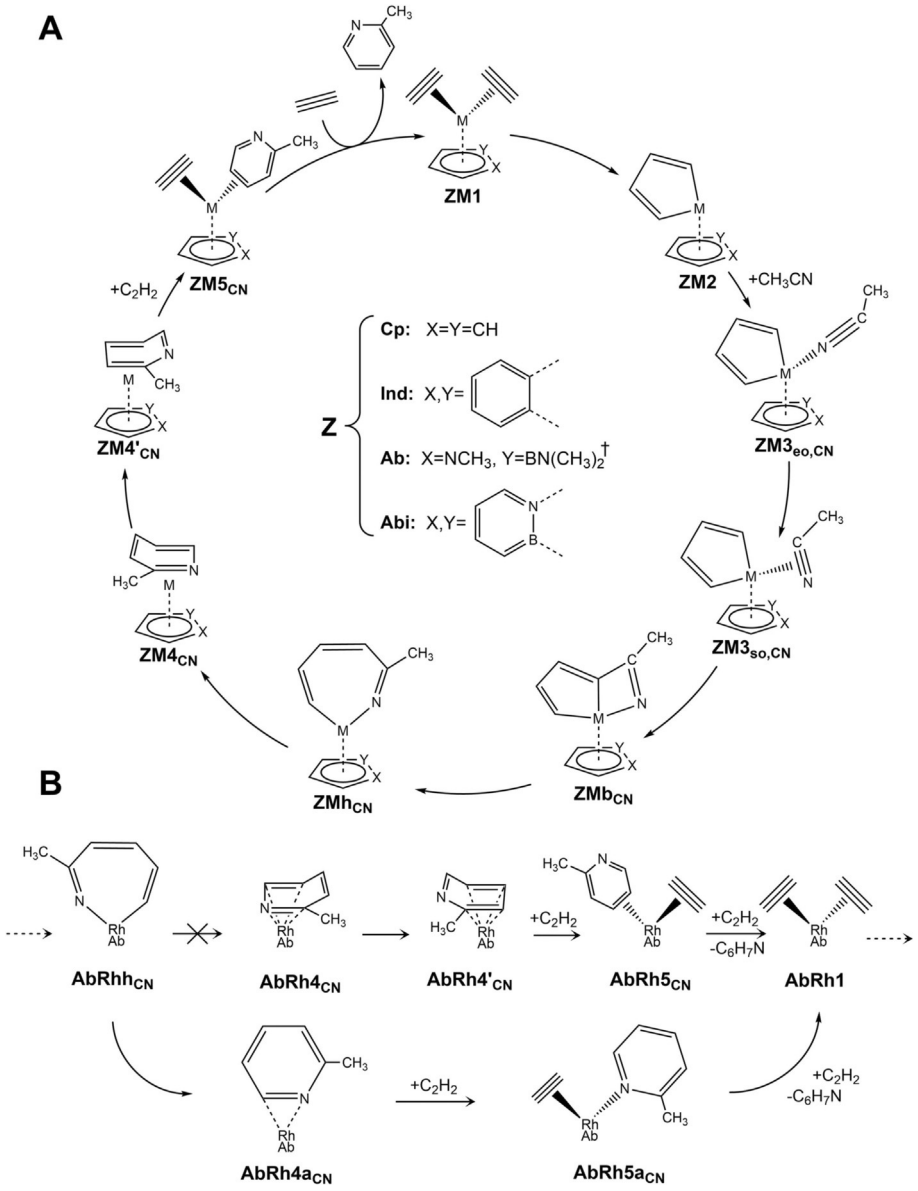

Scheme 4. A) Mechanism for the [2+2+2] cycloaddition of acetylene/acetonitrile to give 2-methylpyridine catalyzed by a half-sandwich metal fragment CpM (M = Co, Rh) and ZRh. †Only up to ZMh_{CN}, then the cycle proceeds as shown in panel (B). B) Final part of the mechanism for the [2+2+2] cycloaddition of acetylene/acetonitrile to give 2-methylpyridine catalyzed by the AbRh fragment starting from the heptacyclic intermediate $AbRhh_{CN}$.

bonds to the metal center in a σ fashion and without any appreciable energy barrier to form an end-on complex ($ZM3_{eo,CN}$); then, upon rotation of the nitrile fragment, overlap between the metal d orbitals and the CN π system increases and $ZM3_{so,CN}$ forms. This linkage isomerism leading to side-on coordination of CH_3CN requires an activation energy and was systematically studied in silico in 2008.[30] Starting from the activated side-on structure and passing through $TS(ZM3_{so,CN},ZMb_{CN})$, the bicyclic complex ZMb_{CN} forms. Then, the hinge metal–carbon bond is weakened along the reaction coordinate, and the heptacyclic structure ZMh_{CN} forms; despite being coordinatively unsaturated, this is a very stable intermediate due to the high exothermic step. Then, reductive elimination leads to the formation of $ZM4_{CN}$, in which newly formed 2-methylpyridine is coordinated to the metal in an η^4 fashion by using four carbon atoms. Fast isomerization to the new η^4 structure $ZM4'_{CN}$ occurs. The new CCNC-bonded structure, located after the transition state $TS(ZM4_{CN},ZM4'_{CN})$, is more stable than the initial CCCC-bonded one. The addition of an acetylene molecule helps to lower the hapticity of the planar pyridine derivative from η^4 to η^2 in the last structure $ZM5_{CN}$. Complete removal of the product to the reaction environment is promoted by the addition of a second acetylene molecule, and the initial catalyst is regenerated.

For comparison, Figure 2A also includes the CpCo-catalyzed cycle computed at a different level of theory (black dashed line), that is, B3LYP combined with the 6-31G(d,p) basis set for all elements.[31]

All intermediates and transition states sketched in Scheme 4 have successfully been located on the PES with one exception in AbRh catalysis. In fact, for the AbRh catalyst, the same mechanistic path as that shown in Scheme 4 is followed, but only until the formation of the heptacyclic intermediate $AbRhh_{CN}$. The next transition state does not lead to the formation of a complex with an η^4-coordinated 2-methylpyridine but instead directly leads to the formation of a product with an η^2-coordinated 2-methylpyridine ($AbRh4a_{CN}$) bonded with a nitrogen atom and a carbon atom to the metal center (Scheme 4B). The last step is barrierless and ends with the formation of a σ bond between the metal and the N atom of 2-methylpyridine upon coordination of an acetylene molecule ($AbRh5a_{CN}$). From this intermediate, the cycle switches back again to AbRh1 after 2-methylpyridine cleavage is promoted by the addition of a second acetylene molecule. For this reason, the PES of the AbRh cycle is not included in Figure 2A but is shown separately in Figure 2B.[40]

2.3. TOF Calculations

Generally, in organometallic catalysis, the most used parameter to measure how many moles of substrate are required to reach the catalyst's saturation is the turnover number (TON). However, it is usually convenient to turn this value into a time-dependent parameter, that is, the turnover frequency, which is the turnover number per unit of time. After generating the PESs, we calculated the TOFs of the catalytic cycles, as explained in the Computational Methods section.

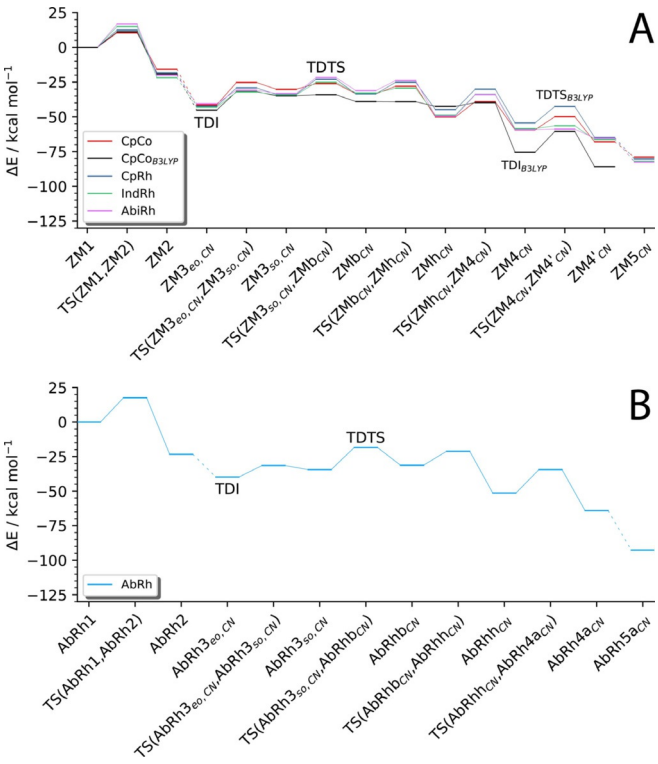

Figure 2. A) Energy profile for the metal-catalyzed [2+2+2] cycloaddition of acetylene/acetonitrile to give 2-methylpyridine (level of theory: ZORA-BLYP/TZ2P). The dashed black line was drawn by using data taken from Ref. [31] computed at a different level of theory, that is, B3LYP/6-31G(d,p). The mechanism is shown in Scheme 4A. B) Energy profile for the AbRh-catalyzed [2+2+2] cocycloaddition of acetylene/acetonitrile to give 2-methylpyridine. The alternative reaction path begins from $AbRhh_{CN}$ and is shown in Scheme 4B.

To approach the experimental conditions in the TOF calculations, we chose two reference temperatures: the first one was the IUPAC standard room temperature (25°C) and the second one was the reflux temperature of toluene, 110.6°C, sometimes used as a solvent in cyclotrimerization reactions.[24]

First, we discuss the [2+2+2] cycloaddition of acetylene to give benzene mediated by different catalysts. In all cases, the TOF-determining intermediate (TDI) is the bis-acetylene intermediate, and the TOF transition state (TDTS) is the subsequent transition state leading to the five-membered ring metallacycle. The crucial step of the whole cycle is indeed oxidative coupling, as the degree of TOF control is almost one for all the analyzed catalysts. For this reason, a dedicated analysis of these species was recently performed.[34] CpCo has the highest efficiency (Table 1), in agreement with the experimental findings. CpIr is somewhat less performant, followed by CpRh. A less extended aromatic ligand (Cp anion) seems to be a better choice than polycyclic moieties, such as Ind. The asymmetric diheteroaromatic fragments (AbRh and AbiRh) are, in general, the worst catalysts, and their chemical activities are more or less comparable.

Notably, no indenyl effect[41] is found, that is, no enhancement in reactivity is achieved by using IndRh rather than CpRh, as predicted in 2007.[29] In contrast, a mild indenyl effect is

Table 1. Calculated TOF values and TOF ratios[a] for the catalytic cycle of Scheme 2I ([2+2+2] cycloaddition of acetylene to give benzene).

Catalyst	$TOF_{298.15\,K}$ [s^{-1}]	$Ratio_{298.15\,K}$	$TOF_{383.65\,K}$ [s^{-1}]	$Ratio_{383.65\,K}$
CpCo	1.3×10^{5}	144928	8.6×10^{6}	12464
CpIr	6.9×10^{4}	100000	5.1×10^{6}	7391
CpRh	4.4×10^{3}	6377	6.2×10^{5}	899
IndRh	5.4×10^{1}	78	2.0×10^{4}	29
AbiRh	3.1×10^{0}	4	2.2×10^{3}	3
AbRh	6.9×10^{-1}	1	6.9×10^{2}	1

[a] TOF ratio = TOF(catalyst)/TOF(AbRh).

present with the diheteroaromatic catalysts, considering that AbRh and AbiRh are structurally analogous to CpRh and IndRh, respectively. The lack of an indenyl effect was recently explained in the hypothesis that an ancillary CO ligand remains bonded to Rh throughout the whole catalytic cycle.[35] The TOF values were also calculated for these cycles (Table 2), and the Ind-based catalyst is ten orders of magnitude more efficient than the Cp-based one.

Table 2. Calculated TOF values and TOF ratios[a] for the catalytic cycle of Scheme 3 ([2+2+2] cycloaddition of acetylene to give benzene).

Catalyst	$TOF_{298.15\,K}$ [s^{-1}]	$Ratio_{298.15\,K}$	$TOF_{383.65\,K}$ [s^{-1}]	$Ratio_{383.65\,K}$
CO-IndRh	7.1×10^{-9}	5.5×10^{10}	4.3×10^{-4}	2.3×10^{8}
CO-CpRh	1.3×10^{-19}	1	1.9×10^{-12}	1

[a] TOF ratio = TOF(catalyst)/TOF(CO-CpRh).

The TOFs for the [2+2+2] cocyclotrimerization of acetylene/acetonitrile to 2-methylpyridine were computed as well (Table 3). A change in the metal implies a significant variation in efficiency, as previously shown in Table 1 for the cyclotrimerization of acetylene. Also, the trend is retained: CpCo works better than Rh-based catalysts. In this case, on the basis of the degree of TOF control, the TDI is the end-on adduct ($ZM3_{eo,CN}$), and the TDTS is the transition state between the species with side-on coordination of the acetonitrile and the bicyclic intermediate, TS($ZM3_{so,CN}$, ZMb_{CN}). This applies to all tested catalysts except CpCo. The energetics of the first CpCo-catalyzed cycle was computed by Dahy et al.[31] with the B3LYP hybrid functional. On their PES, we found that the TDI is the product of the reductive elimination of the heptacycle once the first tetrahapto-bonded pyridine molecule is formed ($CpCo4_{CN}$). The TDTS lies between the two intermediates characterized by η^4-coordinated 2-methylpyridines, that is, TS($CpCo4_{CN}$, $CpCo4'_{CN}$). The CpCo-catalyzed cycle computed in the present work by using ZORA-BLYP/TZ2P identifies the TDTS mainly in correspondence of the end-on/side-on interconversion (80%) and the remaining part on the previously reported TS($ZM3_{so,CN}$, ZMb_{CN}) (20%). The TDI corresponds to the intermediate with the end-on-bonded acetonitrile ($ZM3_{eo,CN}$).

Table 3. Calculated TOF values and ratios[a] for the cocyclotrimerization of acetylene/acetonitrile to give 2-methylpyridine.

Catalyst	$TOF_{298.15\,K}$ [s^{-1}]	$Ratio_{298.15\,K}$	$TOF_{383.65\,K}$ [s^{-1}]	$Ratio_{383.65\,K}$
$CpCo_{B3LYP}$	5.8×10^{1}	1450	2.0×10^{4}	282
CpCo	6.4×10^{0}	160	3.4×10^{3}	48
IndRh	4.0×10^{-1}	10	4.2×10^{2}	6
AbiRh	8.2×10^{-2}	2	1.2×10^{2}	2
CpRh	4.0×10^{-2}	1	7.1×10^{1}	1
AbRh	1.2×10^{-3}	–	4.7×10^{0}	–

[a] TOF ratio = TOF(catalyst)/TOF(CpRh).

This latter case is an instructive example of a situation in which the results from the energy span approximation [Eq. (8)] may be misinterpreted. Thus, here, it is not possible to univocally identify the TDTS, and this prevents a straightforward definition of a correct energy span to be used in Equation (8). To avoid errors in the TOF calculations, in all cases we used the complete equation [Eq. (6)] without any approximation. The performance improvement can also be readily seen from the energy profiles (Figure 2A), for which, relative to the other cycles, the CpCo one is much flatter. This follows a rather common rule of thumb that is used in catalysis: if a reaction involves small energy variations, it usually implies that the cycle is characterized by very high reaction rates.

In 2-methylpyridine formation, a slight indenyl effect is present: IndRh is ten times more efficient than CpRh. The performance of AbiRh is mostly comparable to that of CpRh (at both temperatures). AbRh TOF values cannot be compared, as the reaction mechanism shows some significant differences in the final stages.

2.4. Slippage: A Novel Metal Decentralization Marker

The studied catalysts, in which the aromatic hydrocarbon ligand is the six-electron Cp anion or the ten-electron Ind ligand, have intriguing electronic and structural properties. In fact, the coordination of the metal to the ring is not perfectly symmetric (η^5) but can be described as a distorted arrangement, in which the five metal–carbon distances are not equal: two distances are shorter (M–C1 and M–C3) and two distances are longer (M–C1a and M–C3a), as shown in Scheme 5. Typically, one carbon atom (C2) is found between those at a closer distance, and it may be located below the ring plane, so that a folding angle can be observed. This tipped structure, described as $\eta^3+\eta^2$, is related to the phenomenon known as metal slippage. Further distortion can lead to allylic coordination (η^3) and, in extremis, to the formation of a σ bond between the metal and one C atom (η^1). To quantify the amount of slippage, a parameter was introduced,[42] defined as [Eq. (1)]:

$$\Delta\,[\text{Å}] = \frac{(M-C1a\ +\ M-C3a)\ -\ (M-C1\ +\ M-C3)}{2} \qquad (1)$$

In Equation (1), M–C1a and M–C3a are the longest distances between M and two adjacent C atoms of the Cp ring and M–C1 and M–C3 are the distances between M and the C atoms

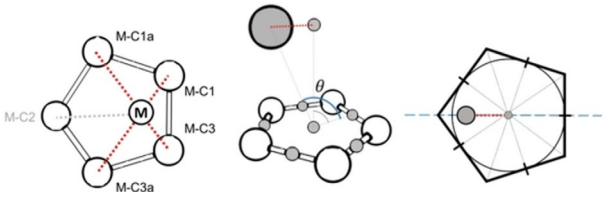

Scheme 5. Novel definition of metal slippage for a five-membered ring.

adjacent to C1a and C3a, respectively. Even without defining rigorous ranges of values to classify metal hapticity, the amount of slippage can be efficiently quantified on the basis of Δ values, which go from 0 (η^5) to about 0.3 (η^3) and to values higher than 0.6 (η^1). Unfortunately, this slippage parameter is partially blind for "out-of-plane" metal displacements. The plane in question (Scheme 2, blue dashed line) is orthogonal to the pseudoplane containing the five-membered-ring atoms. If lateral movement of the metal center takes place, with a consequent irregular variation of the distance pairs M–C1a, M–C3a and M–C1, M–C3, the Δ parameter defined in Equation (1) gives unreliable results. A redefinition of slippage was developed by us mainly for two reasons: to light up every dark corner if C_s symmetry is lost and to build a label-independent parameter to monitor any metal displacement along the reaction coordinate. First, we defined a ring centroid, equal to the center of mass if the five atoms are equal (Cp and Ind), and the middle points of all five bonds between adjacent ring atoms. These points are depicted in gray in Scheme 5.

The label-independent slippage parameter (LISP) was calculated as the sum of the five average minimum distances from a normal vector that passes through the centroid and the metal center (red dotted line, Scheme 2) [Eq. (2)]:

$$\text{LISP [Å]} = \frac{M}{N}\sum_{i=1}^{N}\left|\sin\left(\theta_i - \frac{\pi}{2}\right)\right| \qquad (2)$$

in which M is the distance between the metal atom and the ring centroid; θ_i is the angle between the middle point of two carbon atoms, the ring centroid, and the metal; and N is the number of atoms of the ring. This general definition can be extended in a straightforward manner to five-membered rings containing heteroatoms. As expected, the trend is not significantly different from the Δ values (that preserve an optimal behavior in C_s symmetry for Cp and Ind anions) except if the metal atom drifts out of plane. We chose the average distance to take into account the distortion of the ring from a perfect polygon and to completely untie the label-dependent formalism intrinsic in the definition of Δ.

2.5. Slippage Span Model

The slippage parameter was computed by using the LISP definition for all the intermediates and transition states of the different catalytic cycles. For benzene formation (mechanism of Scheme 2I), the LISP values are shown in Figure 3.

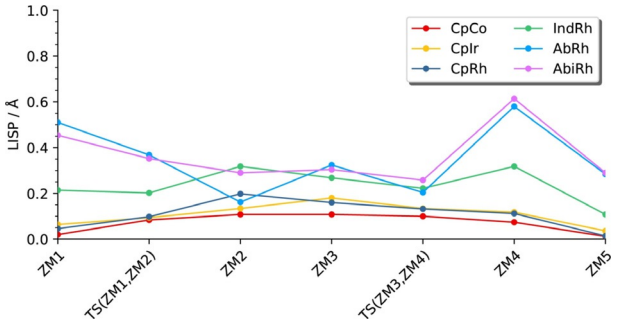

Figure 3. LISP values for the [2+2+2] cyclotrimerization of acetylene to give benzene catalyzed by CpM (M = Co, Rh, Ir) and ZRh (Z = Ind, Ab, Abi). The mechanism is shown in Scheme 2I, and the PESs are shown in Figure 1.

CpM catalysts show a very small variation in LISP along the cycle, especially CpCo; conversely, in the presence of the Ind, Ab, and Abi ligands, higher hapticity variations are computed. To quantify this trend, we introduced a parameter called slippage span (ΔLISP), defined as the difference between the maximum and minimum values of LISP of the whole cycle. The ΔLISP values, for the cases shown in Figure 3, are listed in Table 4.

Table 4. Slippage span values (ΔLISP) and TOF ratios[a] at ambient temperature and in toluene at reflux for the metal-catalyzed [2+2+2] cycloaddition of acetylene to give benzene.

Catalyst	ΔLISP [Å]	TOF ratio 298.15 K	383.65 K
CpCo	0.10	144928	12464
CpIr	0.14	100000	7391
CpRh	0.19	6377	899
IndRh	0.21	78	29
AbiRh	0.36	4	3
AbRh	0.42	1	1

[a] TOF ratio = TOF(catalyst)/TOF(AbRh).

In Table 4, the catalysts are ordered according to decreasing performance. A relationship between geometric and kinetic/energy parameters (TOF ratios) emerges: a lower slippage span ΔLISP corresponds to increased catalytic activity for a given catalyst. A small slippage span ΔLISP is, in general, associated with low absolute LISP values, but the connection between these terms is not straightforward. CpCo is the most rigid fragment: the metal remains almost perfectly centered with respect to the Cp anion during the whole catalytic cycle and only weak slippage occurs. The metal–Cp bonding strength explains the trend of CpIr and CpRh.[34] As expected, IndRh, the intermediates and transition states of which are more slipped and overall show higher flexibility, is less performant than the other catalysts, that is, no indenyl effect is found.

In contrast, a mild indenyl effect is found in the presence of the two diheteroaromatic ligands: AbiRh works better than AbRh; also in these cases, the slippage span follows the trend above described.

The structural information gathered from the ZRh4 intermediate is interesting: in the presence of bulky aromatic ligands, such as Ind, Ab, and Abi, the slippage is very pronounced. The tetrahapto coordination of benzene is likely the cause. In fact, if the benzene molecule switches to an η^2 coordination in the ZRh5 intermediate, the LISP values are dramatically lowered. Notably, the most and the least slipped structures used to calculate ΔLISP do not necessarily match the TDTS and the TDI identified by using Equations (9)–(11). Several reasons can be adduced to explain this unexpected outcome: 1) TDTS and TDI depend on the energetics of all the intermediates and transition states of the catalytic cycle, whereas ΔLISP considers only two structures; 2) the slippage implies an energy change related to the metal–aromatic ring bonding mode, but a larger energy variation is due to the rearrangements occurring in the active part of the complexes; thus, there is necessarily no straight correspondence between the energy profile and the LISP profile; 3) ΔLISP is the easiest but roughest parameter we can consider, as it is not sensitive enough to TOF variations, as explained in the next paragraph.

The important achievement is that minimization of the slippage span leads to an increased catalytic efficiency in terms of TOF values.

To confirm the validity of the slippage span model within different mechanisms, LISP values were also calculated for the [2+2+2] cycloaddition of acetylene catalyzed by CO-CpRh and CO-IndRh, shown in Scheme 3. Very high absolute LISP values were measured on the calculated structures, as remarkable changes in hapticity take place due to the presence of the CO ligand (Figure 4). In fact, the metal center is always slipped far away from the ring centroid, also reaching in some cases η^1 coordination.

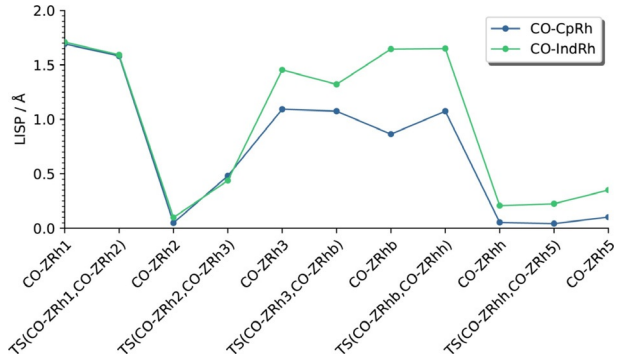

Figure 4. LISP values for the [2+2+2] cycloaddition of acetylene to give benzene catalyzed by CO-CpRh and CO-IndRh. The mechanism is shown in Scheme 3, and the PESs can be found in Ref. [35]

In Table 5, the ΔLISP values for these two cycles are listed with the corresponding TOF ratios. The difference between the ΔLISP values is 0.04 Å for CO-CpRh and CO-IndRh and is comparable to the value obtained in Table 4 for CpRh and IndRh, that is, 0.02 Å. Importantly, the trend is maintained: lower ΔLISP are found in correspondence of higher catalytic performance based on the TOF values.

Table 5. Slippage span values (ΔLISP) and TOF ratios[a] at ambient temperature and in toluene at reflux for CpRh and IndRh in the hypothesis that a CO ligand remains bonded throughout the whole catalytic cycle.

Catalyst	ΔLISP [Å]	TOF ratio 298.15 K	383.65 K
CO-IndRh	1.61	5.5×10^{10}	2.3×10^{8}
CO-CpRh	1.65	1	1

[a] TOF ratio = TOF(catalyst)/TOF(CO-CpRh).

The slippage span model was also tested for the [2+2+2] cocycloaddition of acetylene/acetonitrile to give 2-methylpyridine by using the CpM (M = Co, Rh, Ir) and ZRh (Z = Ind, Abi) catalysts. AbRh was excluded because of mechanistic differences. In Figure 5, CpCo appears again as the most performant, in agreement with the experimental evidence, and as also emerges from the values reported in Table 6. Notably, a mild indenyl effect is found in this mechanism, whereas the CpRh and AbiRh fragments are those with the lowest performance.

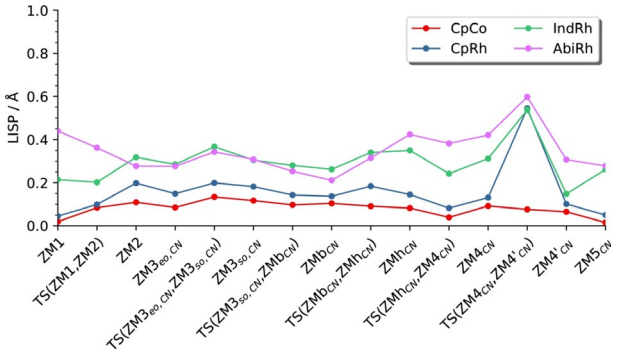

Figure 5. LISP values for the [2+2+2] cocycloaddition of acetylene/acetonitrile to give 2-methylpyridine; the mechanism is shown in Scheme 4 A, and the PESs are shown in Figure 2 A.

Table 6. Slippage span values (ΔLISP) and TOF ratios at ambient temperature and in toluene at reflux for the metal-catalyzed cocyclotrimerization of acetylene/acetonitrile to give 2-methylpyridine.

Catalyst	ΔLISP [Å]	TOF ratio 298.15 K	383.65 K
CpCo	0.12	160	48
IndRh	0.39	10	6
AbiRh	0.39	2	2
CpRh	0.50	1	1

[a] TOF ratio = TOF(catalyst)/TOF(CpRh).

2.6. Improvement of the Slippage Span Model

ΔLISP is a simple way to relate reactivity to a structural parameter, but it seems weak in some critical cases, that is, small ΔLISP values can correspond to large/small differences in the TOF ratios and vice versa. An improved correspondence with variations in the TOF may be achieved by redefining the slippage span with a more complete descriptor that takes into ac-

count all intermediates and transition states rather than considering only the extreme values. This pushed us to work on an extension of the original descriptor ΔLISP. After different trials (Table S5, Supporting Information), the improved slippage span parameter ΔLISP* was introduced [Eq. (3)]. It is the sum of three contributions:

$$\Delta\mathrm{LISP}^*\ [\text{Å}] = \sum_{i=1}^{N-1}|\mathrm{LISP}_1 - \mathrm{LISP}_{i+1}| + \sum_{i=1}^{N-1}|\mathrm{LISP}_i - \mathrm{LISP}_{i+1}| + |\mathrm{LISP}_N - \mathrm{LISP}_1| \quad (3)$$

The first term takes into account how structurally far/close from the starting point every intermediate or transition state of the catalytic cycle is. The second term contains the slippage difference between an arbitrary state and the one immediately following. The last term (third block) is simply the slippage variation between the last intermediate located on the PES and the recovered catalyst. Every term must be as small as possible to have a more efficient catalytic system: in this way, ΔLISP* preserves the same meaning given for the original slippage parameter ΔLISP. A summary of the results is reported in Table 7. At a glance, a great improvement can be noticed upon considering the CO-CpRh and CO-IndRh couple for benzene synthesis and IndRh and AbiRh for the synthesis of 2-methylpyridine. In these two cases, the sensitivity issues found with ΔLISP are nicely solved with ΔLISP*.

Notably, ΔLISP* is constructed in such a way that it does not depend only on the least and most slipped structures encountered in the catalytic cycles; rather, it is a function of the LISPs of all the structures. We cannot identify those two structures controlling the ΔLISP* value, in analogy with TDTS and TDI, because we do not have equations analogous to Equations (9)–(11), that is, we do not have an expression for ΔLISP* as a function of the energies of all the intermediates and transition states of the catalytic cycle. Nevertheless, we analyzed the terms of Equation (3) and their values (see Tables S6 and S7). In general, all structures contribute to ΔLISP*, and in all cases, except one,[43] more than two structures have similar weight, precluding the identification of two slippage span-determining intermediates/transition states.

Table 7. TOF ratios,[a] slippage span values (ΔLISP), and improved slippage span values (ΔLISP*) for benzene and pyridine synthesis.

Catalyst	TOF ratio$_{298.15\,K}$	ΔLISP [Å]	ΔLISP* [Å]
Benzene synthesis			
CpCo	144928	0.10	0.58
CpIr	100000	0.14	0.66
CpRh	6377	0.19	0.88
IndRh	78	0.21	1.02
AbiRh	4	0.36	2.00
AbRh	1	0.42	2.81
CO-IndRh	5.5×10^{10}	1.61	14.48
CO-CpRh	1	1.65	16.31
2-Methylpyridine synthesis			
CpCo	160	0.12	1.34
IndRh	10	0.39	2.76
AbiRh	2	0.39	3.04
CpRh	1	0.50	3.14

[a] For benzene synthesis, TOF ratio = TOF(catalyst)/TOF(AbRh) or TOF(catalyst)/TOF(CO-CpRh). For 2-methylpyridine synthesis, TOF ratio = TOF(catalyst)/TOF(CpRh).

3. Conclusions

Herein, we developed the slippage span model, which establishes a quantitative relationship between, on the one hand, the extent of variation in the geometrical slippage along the reaction of the metal relative to its aromatic ligand in group 9 metal half-sandwich complexes and, on the other hand, their catalytic activity in the [2+2+2] cycloaddition of alkynes. Our computed turnover frequencies (TOFs) of the catalytic cycles for the cyclotrimerization of acetylene to benzene show that Co catalysts perform better than Rh and Ir ones. This trend originates from the first reaction step, oxidative coupling, which involves both the TOF-determining intermediate (TDI) and the TOF-determining transition state (TDTS). Indeed, in this elementary step, the more rigid and, thus, almost perfectly η^5 CpCo complex is more efficient than the more slipped $\eta^3+\eta^2$ CpRh and CpIr complexes.[34]

On the other hand, an indenyl effect was found upon comparing the CpRh and IndRh catalysts in the cocyclotrimerization of acetylene/acetonitrile to 2-methylpyridine and in the cyclotrimerization of acetylene to benzene only if the CO-CpRh and CO-IndRh catalysts were used, that is, for cycles in which the intermediates and transition states possess no symmetry. Conversely, upon comparing the CpRh- and IndRh-catalyzed cyclotrimerization of acetylene to benzene, in which almost all intermediates and transition states have pseudo-C_s symmetry, no indenyl effect was predicted.

Our results point out that lowering the molecular symmetry, through significant hapticity deviations from ideal η^5, reduces the catalyst's performance. This suggests the existence of a relationship between reactivity and metal slippage, which is the essence of the proposed slippage span model. We defined a new slippage parameter, the label-independent slippage parameter (LISP), which is also valid for and applicable to non-symmetric metal displacements. Our computations revealed an inverse trend upon comparing the TOF and ΔLISP values, that is, the slippage span or difference between the maximum and minimum LISP values along a catalytic cycle. This outcome was even more evident upon using the improved ΔLISP*, which takes into account the hapticities of all the intermediates and transition states of the catalytic cycle. The proposed slippage span model can serve as a guideline for the rational design of a performant half-sandwich, group 9 metal catalyst for [2+2+2] cycloadditions.

Computational Details

All DFT calculations were performed with the Amsterdam Density Functional (ADF) program.[44–46] The zeroth-order regular approximation (ZORA)[47] was used to account for scalar relativistic effects. The BLYP exchange and correlation functional, developed by

Becke[48] (exchange part) and Lee, Yang, and Parr[49–51] (correlation term), was used in combination with the TZ2P basis set for all elements. The TZ2P basis set is a large uncontracted set of Slater-type orbitals (STOs) that was slightly optimized to fit the best results with the applied scalar relativistic Hamiltonian. It is of triple-ζ quality and is augmented with two sets of polarization functions on each atom: 2p and 3d in the case of H, 3d and 4f in the case of C and N, 4p and 4f in the case of Co, 5p and 4f in the case of Rh, and 6p and 5f in the case of Ir. A small frozen-core approximation was also employed: up to 1s for C and N, up to 2p for Co, up to 3d for Rh, and up to 4d for Ir. To analyze the performance of our catalysts, we investigated the potential energy surface of the process by computing the geometries of the intermediates and transition states and their relative energies. Minimum energy and transition-state geometries were optimized without any symmetry constraint by using analytical-gradient techniques. Frequency calculations were performed to verify that minima had all positive frequencies, whereas transition states had a single negative frequency; the character of the normal mode associated to the negative frequency was analyzed to ensure that the correct transition state was found.

Turnover Frequency (TOF) Calculations

The turnover frequency (TOF) is a valuable parameter to better understand and characterize the analyzed catalyst. In the beginning, it was conceived to describe enzymatic kinetics and biological promotor/inhibitor species, but the TOF concept can be extended to any cyclic reaction. The canonical definition of TOF is [Eq. (4)]:

$$\mathrm{TOF} = \frac{N}{t} \tag{4}$$

in which t is the total time required to perform N cycles or to create N molecules of product. A modern approach aiming at translating thermodynamic data into kinetics is the definition of the energy span,[52] as the difference between the energy of the highest energy transition state and the energy of the lowest intermediate to establish a relation between the classical Arrhenius equation and the Boltzmann distribution. Unluckily, this formulation gives exact results only if the energy of the starting reactants lies at the same energy level of the final products, that is, $\Delta G_r^\circ = 0$. Kozuch and Shaik proposed a more general model to calculate the TOF on the basis of Christianen's idea:[53] they defined the turnover frequency directly in terms of the summation of the kinetic constants. By implementing the Eyring transition-state theory (TST) with the Eyring–Polanyi equation [Eq. (5)]:

$$k = \frac{k_B T}{h} e^{\frac{-\Delta G^{\ddagger}}{RT}} \tag{5}$$

in which k_B is Boltzmann's constant, T is the temperature, h is Planck's constant, and R is the universal gas constant, they succeeded in deriving the expression [Eq. (6)]:[54]

$$\mathrm{TOF} = \frac{k_B T}{h} \frac{e^{\frac{-\Delta G_r}{RT}} - 1}{\sum_{i,j=1}^{N} e^{(T_i - I_j - \delta G_{i,j})/RT}} = \frac{\Delta}{M} \tag{6}$$

for which [Eq. (7)]:

$$\delta G_{i,j} = \begin{cases} \Delta G_r & \text{if} \quad i > j \\ 0 & \text{if} \quad i \le j \end{cases} \tag{7}$$

in which T_i and I_j indicate the Gibbs free energies of the i^{th} transition state and j^{th} intermediate, respectively. Equation (6) has analogy with Ohm's first law: TOF is a reactants/products flux (in analogy with current intensity), Δ is analogous to the electric potential difference, and M can be interpreted as a resistance due to the reactant's flux. Importantly, in this model, the energy differences between all intermediates and all transition states are considered. In fact, the denominator is a summation of N^2 exponential terms for each index permutation. The numerator overcomes the limitation above mentioned, as ΔG_r is the difference between the free energies of the products and the reactants. Overall, all the elementary steps of the catalytic cycle are included in the definition of the TOF, and so the rate-determining step (RD step) concept fades into the rate-determining states (RD states) concept, which represents a flexible and accurate way to analyze the efficiency of a cyclic process. This model relies on three assumptions: 1) Eyring TST is used; 2) Bodenstein's approximation, better known as steady-state regime, must be true; 3) all stationary points undergo fast thermal equilibration with their surroundings.

In many catalytic cycles, Equation (6) can be simplified by: 1) neglecting the "−1" term in the numerator: it is merely introduced to avoid thermodynamic inconsistencies for endergonic (TOF < 0) or close-to-equilibrium reactions (TOF = 0). This term becomes unimportant in exergonic cycles; 2) limiting the denominator to a single exponential term: only the term that involves the two TOF-determining states is dominant and must be retained in the expansion; all the rest becomes negligible.

On this basis, Equation (6) can be written as [Eq. (8)]:

$$\mathrm{TOF} \approx \frac{k_B T}{h} e^{(I_{\mathrm{TDI}} - T_{\mathrm{TDTS}} - \delta G_{\mathrm{TDI,TDTS}})/RT} = \frac{k_B T}{h} e^{-\delta E/RT} \tag{8}$$

in which I_{TDI} and T_{TDTS} are the Gibbs free energies of the TOF-determining intermediate (TDI) and TOF-determining transition state (TDTS), respectively; δE is called energy span.

The identification of the TDI and TDTS in a catalytic cycle is based on an elegant technique that determines the variations in the TOF in direct relation with the energy variation in one TS/intermediate. In analogy with the definition of degree of rate control (RC), Kozuch and Shaik derived [Eq. (9)]:[54]

$$X_{\mathrm{RC},i} = \frac{k_i}{r}\left(\frac{\partial r}{\partial k_i}\right)_{k_{i\neq j},K} \rightarrow X_{\mathrm{TOF},i} = \left|\frac{1}{\mathrm{TOF}}\frac{\partial \mathrm{TOF}}{\partial E_i}\right| \tag{9}$$

in which r is the overall reaction rate and k_i is the constant rate for the i^{th} step. The identities of Equation (9) are [Eqs. (10) and (11)]:

$$X_{\mathrm{TOF},T_i} = \frac{\sum_{j=1}^{N} e^{(T_i - I_j - \delta G_{i,j})/RT}}{\sum_{i,j=1}^{N} e^{(T_i - I_j - \delta G_{i,j})/RT}} \tag{10}$$

$$X_{\mathrm{TOF},I_j} = \frac{\sum_{i=1}^{N} e^{(T_i - I_j - \delta G_{i,j})/RT}}{\sum_{i,j=1}^{N} e^{(T_i - I_j - \delta G_{i,j})/RT}} \tag{11}$$

The bigger the degree of TOF control (X_{TOF}), the higher the impact of the energy variation of the considered state on the TOF. With this mathematical strategy, both TDI and TDTS are quickly identified for a particular catalytic cycle.

It is important to stress that RD step theory fails to predict a few delicate but important aspects that rule the efficiency of a catalyst. An example is the presence in the cycle of some very low energy species: the resulting effect is quenching of the catalyst (trapped in a potential well) with a dramatic drop in terms of activity. The RD step approach does not describe adequately these situations, because it is focused on the so common "highest limiting barrier" or "lowest kinetic rate step" concepts.

In principle, all the energies in Equations (5)–(11) must be Gibbs free energies. Given that our purpose was to compare different catalysts with identical mechanisms, the TOF ratio is a meaningful value. In fact, it benefits from a large error compensation and electronic energies can be used, as entropic contributions are likely very similar in analogous mechanisms.[35]

Acknowledgements

All the calculations were performed on Galileo (CINECA: Casalecchio di Reno, Italy). Principal Investigator L.O. acknowledges CINECA for computational budget on the Italian SuperComputing Resource Allocation (ISCRA) Grant STREGA (Filling the STructure–REactivity GAp: in silico multiscale approaches to rationalize the design of molecular catalysts). M.D.T. is grateful to Fondazione CARIPARO for financial support (Ph.D. grant). L.O. acknowledges Università degli Studi di Padova (BIRD2018) for financial support. F.M.B. thanks the Netherlands Organization for Scientific Research (NWO) for financial support.

Conflict of Interest

The authors declare no conflict of interest.

Keywords: cycloadditions · density functional calculations · half-metallocenes · reaction mechanisms · slippage span

[1] K. Tanaka, *Transition-Metal-Mediated Aromatic Ring Construction*, Wiley, Hoboken, NJ, **2013**.
[2] G. Schmid, M. Schütz, *Organometallics* **1992**, *11*, 1789 – 1792.
[3] G. Schmid, M. Schütz, *J. Organomet. Chem.* **1995**, *492*, 185 – 189.
[4] G. Schmid, B. Kilanowski, R. Boese, D. Bläser, *Chem. Ber.* **1993**, *126*, 899 – 906.
[5] G. Schmid, R. Boese, *Z. Naturforsch. B* **1983**, 485 – 492.
[6] G. Schmid, S. Amirkhalili, U. Höhner, D. Kampmann, R. Boese, *Chem. Ber.* **1982**, *115*, 3830 – 3841.
[7] G. Schmid, D. Kampmann, U. Höhner, D. Bläser, R. Boese, *Chem. Ber.* **1984**, *117*, 1052 – 1060.
[8] G. Schmid, F. Schmidt, *Chem. Ber.* **1986**, *119*, 1766 – 1771.
[9] G. Schmid, D. Kampmann, W. Meyer, R. Boese, P. Paetzold, K. Delpy, *Chem. Ber.* **1985**, *118*, 2418 – 2428.
[10] S.-Y. Liu, M. M.-C. Lo, G. C. Fu, *Angew. Chem. Int. Ed.* **2002**, *41*, 174 – 176; *Angew. Chem.* **2002**, *114*, 182 – 184.
[11] A. J. Ashe, X. Fang, *Org. Lett.* **2000**, *2*, 2089 – 2091.
[12] A. J. Ashe, X. Fang, X. Fang, J. W. Kampf, *Organometallics* **2001**, *20*, 5413 – 5418.
[13] X. Fang, H. Yang, J. W. Kampf, M. M. Banaszak Holl, A. J. Ashe, *Organometallics* **2006**, *25*, 513 – 518.
[14] J. H. Hardesty, J. B. Koerner, T. A. Albright, G.-Y. Lee, *J. Am. Chem. Soc.* **1999**, *121*, 6055 – 6067.
[15] W. Reppe, O. Schlichting, K. Klager, T. Toepel, *Justus Liebigs Ann. Chem.* **1948**, *560*, 1 – 92.
[16] Y. Wakatsuki, H. Yamazaki, *J. Chem. Soc. Chem. Commun.* **1973**, 280a.
[17] Y. Wakatsuki, H. Yamazaki, *Bull. Chem. Soc. Jpn.* **1985**, *58*, 2715 – 2716.
[18] K. P. C. Vollhardt, *Acc. Chem. Res.* **1977**, *10*, 1 – 8.
[19] K. P. C. Vollhardt, *Angew. Chem. Int. Ed. Engl.* **1984**, *23*, 539 – 556; *Angew. Chem.* **1984**, *96*, 525 – 541.
[20] H. Bönnemann, *Angew. Chem. Int. Ed. Engl.* **1978**, *17*, 505 – 515; *Angew. Chem.* **1978**, *90*, 517 – 526.
[21] H. Bönnemann, *Angew. Chem. Int. Ed. Engl.* **1985**, *24*, 248 – 262; *Angew. Chem.* **1985**, *97*, 264 – 279.
[22] J. P. Collman, J. W. Kang, W. F. Little, M. F. Sullivan, *Inorg. Chem.* **1968**, *7*, 1298 – 1303.
[23] K. Abdulla, B. L. Booth, C. Stacey, *J. Organomet. Chem.* **1985**, *293*, 103 – 114.
[24] P. Cioni, P. Diversi, G. Ingrosso, A. Lucherini, P. Ronca, *J. Mol. Catal.* **1987**, *40*, 337 – 357.
[25] P. Diversi, L. Ermini, G. Ingrosso, A. Lucherini, *J. Organomet. Chem.* **1993**, *447*, 291 – 298.
[26] A. W. Fatland, B. E. Eaton, *Org. Lett.* **2000**, *2*, 3131 – 3133.
[27] L. Yong, H. Butenschön, *J. Chem. Soc. Chem. Commun.* **2002**, 2852 – 2853.
[28] K. Kirchner, M. J. Calhorda, R. Schmid, L. F. Veiros, *J. Am. Chem. Soc.* **2003**, *125*, 11721 – 11729.
[29] L. Orian, J. N. P. van Stralen, F. M. Bickelhaupt, *Organometallics* **2007**, *26*, 3816 – 3830.
[30] L. Orian, W. J. van Zeist, F. M. Bickelhaupt, *Organometallics* **2008**, *27*, 4028 – 4030.
[31] A. A. Dahy, K. Yamada, N. Koga, *Organometallics* **2009**, *28*, 3636 – 3649.
[32] C.-H. Guo, H.-S. Wu, M. Hapke, H. Jiao, *J. Organomet. Chem.* **2013**, *748*, 29 – 35.
[33] A. A. Dahy, N. Koga, *Organometallics* **2015**, *34*, 4965 – 4974.
[34] M. Dalla Tiezza, F. M. Bickelhaupt, L. Orian, *ChemPhysChem* **2018**, *19*, 1766 – 1773.
[35] L. Orian, M. Swart, F. M. Bickelhaupt, *ChemPhysChem* **2014**, *15*, 219 – 228.
[36] N. E. Schore, *Chem. Rev.* **1988**, *88*, 1081 – 1119.
[37] A. A. Dahy, C. H. Suresh, N. Koga, *Bull. Chem. Soc. Jpn.* **2005**, *78*, 792 – 803.
[38] L. Orian, L. P. Wolters, F. M. Bickelhaupt, *Chem. Eur. J.* **2013**, *19*, 13337 – 13347.
[39] G. Dazinger, M. Torres-Rodrigues, K. Kirchner, M. J. Calhorda, P. J. Costa, *J. Organomet. Chem.* **2006**, *691*, 4434 – 4445.
[40] All the calculations were performed in the gas phase. To take into account solvation, we used the COnductor-like Screening MOdel (COSMO).[55] The chosen solvents were toluene, a very common aprotic medium, and acetonitrile, which is one of the reactants for the synthesis of 2-methylpyridine. Single-point energy corrections with COSMO were computed by using the geometries optimized in the gas phase. This was possible after checking that our molecular structures were almost unaffected if embedded in the solvent.[56] In both solvents, the result was an overall stabilization of the entire PES, as can be seen in Figures S1 – S3. Acetonitrile led to the largest change in energies (a larger stabilization), whereas toluene showed milder stabilization of the stationary points, in line with the dielectric constants of the two solvents. The energy shift was almost constant for every intermediate and transition state. Thus, we concluded that the solvent effects on the energy profiles could be disregarded for the analyzed processes. The main reason for this was the absence of strongly polarized and charged species.
[41] M. E. Rerek, F. Basolo, *J. Am. Chem. Soc.* **1984**, *106*, 5908 – 5912.
[42] M. E. Rerek, L.-N. Ji, F. Basolo, *J. Chem. Soc. Chem. Commun.* **1983**, 1208 – 1209.
[43] In the AbRh-catalyzed cycloaddition of acetylene/acetonitrile to give 2-methylpyridine, a very large LISP variation occurs if the pyridine ring changes its bonding mode to the metal, very likely for strong steric effects, and although this does not imply an energy variation larger than the preceding steps, a sharp spike appears in the LISP profile of the cycle.
[44] C. Fonseca Guerra, J. G. Snijders, G. te Velde, E. J. Baerends, *Theor. Chem. Acc.* **1998**, *99*, 391 – 403.
[45] G. te Velde, F. M. Bickelhaupt, E. J. Baerends, C. Fonseca Guerra, S. J. A. van Gisbergen, J. G. Snijders, T. Ziegler, *J. Comput. Chem.* **2001**, *22*, 931 – 967.

[46] E. J. Baerends, T. Ziegler, A. J. Atkins, J. Autschbach, D. Bashford, O. Baseggio, A. Bérces, F. M. Bickelhaupt, C. Bo, P. M. Boerritger, L. Cavallo, C. Daul, D. P. Chong, D. V. Chulhai, L. Deng, R. M. Dickson, J. M. Dieterich, D. E. Ellis, M. van Faassen, A. Ghysels, A. Giammona, S. J. A. van Gisbergen, A. Goez, A. W. Götz, S. Gusarov, F. E. Harris, P. van den Hoek, Z. Hu, C. R. Jacob, H. Jacobsen, L. Jensen, L. Joubert, J. W. Kaminski, G. van Kessel, C. König, F. Kootstra, A. Kovalenko, M. Krykunov, E. van Lenthe, D. A. McCormack, A. Michalak, M. Mitoraj, S. M. Morton, J. Neugebauer, V. P. Nicu, L. Noodleman, V. P. Osinga, S. Patchkovskii, M. Pavanello, C. A. Peeples, P. H. T. Philipsen, D. Post, C. C. Pye, H. Ramanantoanina, P. Ramos, W. Ravenek, J. I. Rodríguez, P. Ros, R. Rüger, P. R. T. Schipper, D. Schlüns, H. van Schoot, G. Schreckenbach, J. S. Seldenthuis, M. Seth, J. G. Snijders, M. Solà, S. M, M. Swart, D. Swerhone, G. te Velde, V. Tognetti, P. Vernooijs, L. Versluis, L. Visscher, O. Visser, F. Wang, T. A. Wesolowski, E. M. van Wezenbeek, G. Wiesenekker, S. K. Wolff, T. K. Woo, A. L. Yakovlev, *ADF2014*, *ADF2016*, SCM, Theoretical Chemistry, Vrije Universiteit, Amsterdam, The Netherlands.

[47] E. van Lenthe, E. J. Baerends, J. G. Snijders, *J. Chem. Phys.* **1994**, *101*, 9783 – 9792.

[48] A. D. Becke, *Phys. Rev. A* **1988**, *38*, 3098 – 3100.

[49] C. Lee, W. Yang, R. G. Parr, *Phys. Rev. B* **1988**, *37*, 785 – 789.

[50] B. G. Johnson, P. M. W. Gill, J. A. Pople, *J. Chem. Phys.* **1993**, *98*, 5612 – 5626.

[51] T. V. Russo, R. L. Martin, P. J. Hay, *J. Chem. Phys.* **1994**, *101*, 7729 – 7737.

[52] C. Amatore, A. Jutand, *J. Organomet. Chem.* **1999**, *576*, 254 – 278.

[53] J. A. Christiansen, *Adv. Catal.* **1953**, *5*, 311 – 353.

[54] S. Kozuch, S. Shaik, *Acc. Chem. Res.* **2011**, *44*, 101 – 110.

[55] C. C. Pye, T. Ziegler, *Theor. Chem. Acc.* **1999**, *101*, 396 – 408.

[56] L. Orian, A. Bisello, S. Santi, A. Ceccon, G. Saielli, *Chem. Eur. J.* **2004**, *10*, 4029 – 4040.

Received: September 12, 2018

